

Kinetics of Adsorption of the Cobalt Ions on the “Electrolytic Solution/ γ -Alumina” Interface

Theodora Ataloglou,[†] Kyriakos Bourikas,^{†,‡} John Vakros,^{†,‡} Christos Kordulis,^{†,§} and Alexis Lycourghiotis^{*,†}

Department of Chemistry, University of Patras, GR-26500 Patras, Greece, School of Science and Technology, Hellenic Open University, Sahtouri 16, GR-26222 Patras, Greece, and Institute of Chemical Engineering and High-Temperature Chemical Processes, FORTH/ ICE-HT, P.O. Box 1414, GR-26500 Patras, Greece

Received: May 17, 2004; In Final Form: October 20, 2004

In the present work we studied, for the first time, the kinetics of adsorption of the $\text{Co}(\text{H}_2\text{O})_6^{2+}$ species on the “electrolytic solution/ γ - Al_2O_3 ” interface at pH = 7 and 25 °C for a very broad range of Co(II) surface concentrations ranged from 0.03 to 6 theoretical $\text{Co}(\text{H}_2\text{O})_6^{2+}$ surface layers. Moreover, we studied the surface dissolution of γ -alumina in the presence of the $\text{Co}(\text{H}_2\text{O})_6^{2+}$ ions in the impregnating solution, the contribution of the Co(II) desorption on the whole deposition process and the deposition isotherm. It was found that under the conditions where the deposition has taken place, the dissolution of the γ -alumina surface is negligible even in the presence of the $\text{Co}(\text{H}_2\text{O})_6^{2+}$ species in the impregnating solution. It was, moreover, inferred that the Co(II) desorption does not participate significantly to the whole deposition process. It was found that the deposition kinetics may be described by the following kinetic expression $r_{\text{Co,bulk}} = k' C_{\text{Co,bulk}}^2$, which relates the rate of disappearance of the $\text{Co}(\text{H}_2\text{O})_6^{2+}$ ions from the impregnating solution, $r_{\text{Co,bulk}}$, with their concentration $C_{\text{Co,bulk}}$. This kinetic expression may be derived assuming the following deposition scheme: $n\text{S} + 2[\text{Co}(\text{H}_2\text{O})_6^{2+}] \rightarrow \text{S}_n - [\text{Co}(\text{H}_2\text{O})_{x,x<6}^{2+}]_2$, where S represents the surface reception sites. The above expressions indicated that two $\text{Co}(\text{H}_2\text{O})_6^{2+}$ ions are involved, from the side of the interface, in the reaction with the reception sites. It seems probable that the deposition step involves the simultaneous adsorption and dimerization of the two interfacial $\text{Co}(\text{H}_2\text{O})_6^{2+}$ ions through (hydr)oxobridges. On the other hand, the sigmoidal form of the deposition isotherm and the dependence of the apparent rate constant, k' , on the interfacial Co(II) concentration suggested that the already deposited Co(II) species may be involved in the reception sites, S, promoting the adsorption and resulting to the formation of multinuclear complexes and Co(II) surface precipitates. Finally, reasonable interface potential values for oxides were determined for the first time using kinetic results.

Introduction

The study of the deposition of metal ions on the surface of mineral oxides is very useful in many areas including geochemistry, environmental science, water treatment, and colloidal and interface science as well as catalyst preparation. Concerning catalyst preparation the interest is focused on the deposition of the transition metal ionic species (tmis) on the surface of oxides used as supports in heterogeneous catalysis, like γ - Al_2O_3 , α - Al_2O_3 , TiO_2 , and SiO_2 .

It is well-known that supported catalysts containing cobalt in the metallic, oxidic or sulfided state are very important in heterogeneous catalysis.^{1–12} “Equilibrium deposition filtration” (EDF), otherwise called “equilibrium adsorption”, may be used to prepare Co supported catalysts with high Co dispersity and thus an active surface.^{13–19} The achievement of a more severe control of preparation requires the knowledge of the deposition mechanism. This is one of the reasons, among other also important ones, for which several studies in the past had been

focused on this subject.^{20–41} Recently, we have critically reviewed these studies.⁴²

Concerning the methodologies used for studying the adsorption of the $\text{Co}(\text{H}_2\text{O})_6^{2+}$ ions from aqueous solutions on catalytic supports, adsorption experiments have been carried out in most of cases. Moreover, in cases where the charged surface of the support and the interfacial region have been considered, microelectrophoretic mobility and/or potentiometric titration measurements have been performed.^{25,26,32–34} Finally, in certain extremely interesting works EXAFS related techniques have been used.^{22–24,30,31,35,36} It is rather surprising, but to the extent of our knowledge there so far not been reported any systematic kinetic study on the Co deposition on the catalytic supports contributing to the development of a more clear picture for the deposition mechanism. Depending on the state of the art, mainly related to a certain period, the various research groups have adopted, implicitly or explicitly, different surface and interface models to interpret their results. The surface models involved nonelectrostatic approaches^{20,21,37–39} or the homogeneous “one site/two pK” model.^{25,26,28,29,40,41} The heterogeneous and more realistic multisite model has been implied in certain studies.^{27,31,36} However, this model has not been used so far to interpret quantitatively adsorption data. Concerning the interfacial region the triple layer model^{25,26,28,29} or the diffuse layer model^{40,41} has been used to describe the adsorption process.

* To whom correspondence should be addressed. E-mail: kmpo@chemistry.upatras.gr. Telephone: +302610997143. Fax: +302610994796.

[†] University of Patras.

[‡] Hellenic Open University.

[§] Institute of Chemical Engineering and High-Temperature Chemical Processes, FORTH/ ICE-HT.

There is no so far any example illustrating the use of the three plane model^{43,44} and the charge distribution (CD) concept⁴³ of the adsorbed Co(II) species to interpret adsorption.

A detailed examination of the studies reported so far showed that the mechanism of deposition of the $\text{Co}(\text{H}_2\text{O})_6^{2+}$ ions on the surface of catalytic supports depends on two main factors: on the Co(II) surface concentration and on the nature of the support surface.⁴² In this point it should be noticed that the term “Co(II) surface concentration”, used in several places throughout the text, means the total surface concentration of cobalt irrespective of the kind and the number of ligands existing in the inner sphere of cobalt ion.

The first parameter mentioned above, is controlled by regulating the pH, the concentration of the $\text{Co}(\text{H}_2\text{O})_6^{2+}$ ions in the impregnating solution and the impregnation time. The pH of the impregnating solution influences the deposition mechanism but only indirectly, through the change of the Co(II) surface concentration. In fact, it is well established that the increase in the impregnation pH (up to a critical value above which cobalt phases precipitate in the solution) brings about an increase to the extent of deposition and thus to the Co(II) surface concentration.⁴²

It seems that the mechanism changes progressively with the Co(II) surface concentration from the monodentate and/or multidentate-mononuclear inner sphere surface complexes, weakly evidenced in too low values of the Co(II) surface concentration, to multidentate-multinuclear inner sphere surface complexes at relatively low Co(II) surface concentrations, eventually with partial hydrolysis of the Co(II) surface species, and then into a surface $\text{Co}(\text{OH})_2$ -like precipitate at relatively high Co(II) surface concentrations but at pH values lower than those required for bulk precipitation. The general route described above is strongly influenced by the surface characteristics of the support, though in all cases cobalt forms surface species with Co(II) in octahedral symmetry. Moreover, the surface Co(II) inner sphere complexes are formed by exchanging one or more water ligands of the $\text{Co}(\text{H}_2\text{O})_6^{2+}$ ions with the surface oxygens of the support.

Concerning $\gamma\text{-Al}_2\text{O}_3$, the most important catalytic carrier, the few studies reported so far indicated that mononuclear (monodentate or bidentate) or hydrolyzed mononuclear inner sphere Co(II) surface complexes are formed for Co(II) surface concentrations corresponding to a number of theoretical $\text{Co}(\text{H}_2\text{O})_6^{2+}$ surface layers lower than 0.33. Above this value, multinuclear inner sphere Co(II) complexes and surface precipitate are presumably formed. However, according to Tewari and Lee²¹ surface precipitate is formed even at 0.1 theoretical $\text{Co}(\text{H}_2\text{O})_6^{2+}$ surface layers. A quite critical point related to the dependence of the deposition mechanism on the surface characteristics of the support is the sorption behavior of $\gamma\text{-Al}_2\text{O}_3$ with respect to that of SiO_2 and TiO_2 . In fact, Pauliac et al.²³ and Caillerie et al.²⁴ studied the adsorption of $\text{Co}(\text{NH}_3)_6^{2+}$ ions instead of $\text{Co}(\text{H}_2\text{O})_6^{2+}$ ions, on the γ -alumina surface for Co(II) surface concentrations in the region 0.73–1.15 theoretical $\text{Co}(\text{NH}_3)_6^{2+}$ surface layers. They concluded that the surface of γ -alumina is dissolved and the released Al(III) ionic species react with the adsorbed Co(II) ionic species forming a mixed Al–Co precipitate of hydrotalcite structure. Although this deposition mechanism could be taken into account for explaining the relatively high sorption capacity of γ -alumina, as it is compared to that of TiO_2 , it is not so clear that this mechanism actually predominates in the cases where the deposition of Co(II) on γ -alumina takes place through the $\text{Co}(\text{H}_2\text{O})_6^{2+}$ species. For

instance, assuming this mechanism as the predominant one, it is rather difficult to explain the “S” type of the isotherms usually observed.

Although EXAFS and related techniques provided a direct evidence for the formation of inner sphere Co(II) surface complexes on the $\gamma\text{-Al}_2\text{O}_3$ surface,²² much effort is required for elucidating the local structure of the surface complexes even under conditions where mononuclear or oligonuclear inner sphere Co(II) complexes are formed. It is thus necessary the joint use of equilibrium adsorption experiments, electrochemical techniques, kinetic adsorption experiments, spectroscopic results as well as the analysis of the experimental data (including the “metal/proton” exchange ratio) on the base of a multisite model for the $\gamma\text{-Al}_2\text{O}_3$ surface and a charge distribution approach for the interfacial region. However, the application of the multisite model is extremely difficult for $\gamma\text{-Al}_2\text{O}_3$ and simplified assumptions are for the moment necessary.

With the idea to contribute, following the aforementioned approach, to the elucidation of the local structure of the surface Co(II) complexes formed on the $\gamma\text{-Al}_2\text{O}_3$ surface, we attempt in the present work to investigate whether the surface dissolution of the $\gamma\text{-Al}_2\text{O}_3$ and the formation of the mixed Al–Co precipitate of hydrotalcite structure mentioned is the predominant deposition mechanism even in most of cases, where the deposition takes place through the $\text{Co}(\text{H}_2\text{O})_6^{2+}$ ionic species. Moreover, in the present work we study for first time the kinetics of the $\text{Co}(\text{H}_2\text{O})_6^{2+}$ deposition on the γ -alumina surface. The kinetic study is expected to conduct to the determination of the number of the $\text{Co}(\text{H}_2\text{O})_6^{2+}$ ionic species which participate in the rate-determining step of the deposition process taking place in the interfacial region.

Experimental Section

Materials. Cobalt nitrate [$\text{Co}(\text{NO}_3)_3 \cdot 6\text{H}_2\text{O}$, analytical grade] purchased from Merck has been used for the preparation of the solutions used in the adsorption experiments. Ammonium nitrate stock solutions, used as indifferent electrolyte for regulating the ionic strength, were prepared from the respective solid (Merck analytical grade). At this point, it should be mentioned that as indifferent electrolyte is defined an electrolyte the ions of which are not “chemically” adsorbed on the support surface. These are simply retained electrostatically in the outer Helmholtz plane or in the diffuse part of the interfacial region developed between the surface of the support particles and the impregnating solution. γ -Alumina powder, 90–150 μm mesh, was used as adsorbent (support) after drying at 120 °C for 2 h and air-calcination at 600 °C for 12 h. The powder used was obtained by crushing γ -alumina extrudates (AKZO, product code = Drum 1696, $S_{\text{BET}} = 270 \text{ m}^2 \text{ g}^{-1}$, water pore volume = $0.75 \text{ cm}^3 \text{ g}^{-1}$).

Kinetic Adsorption Experiments (Experiments A). The kinetic runs were performed at 25.0 ± 0.1 °C, ionic strength equal to 0.1 M (adjusted by adding ammonium nitrate), and pH equal to 7.0. A double-walled, water-jacketed covered vessel equipped with a pH control system involving a glass saturated calomel electrode (Metrohm) and a dosimat have been used (Figure 1). The aforementioned pH control system allowed the automatic adjustment of pH during the adsorption experiments by adding to the “adsorption vessel” ammonia aqueous solution. Nitrogen gas was passed into the vessel during the adsorption experiments to prevent the dilution of the atmospheric CO_2 , which would bring about a change in the pH.

In each kinetic experiment a volume of 150 mL of cobalt nitrate solution of a given concentration, varying in the range 5×10^{-4} to 2.5×10^{-2} M, and a suitable volume of ammonium

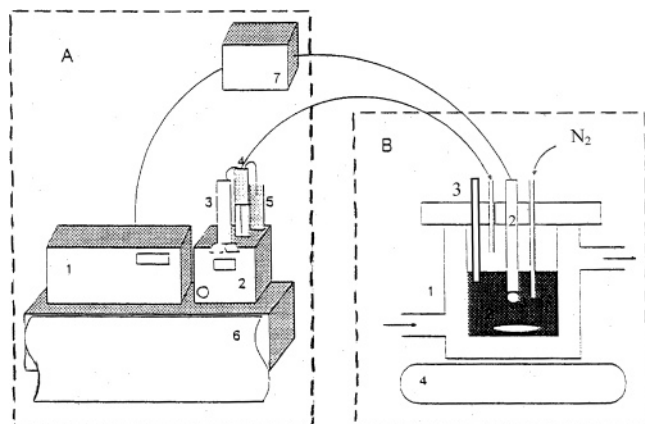


Figure 1. Schematic representation of the experimental setup used to perform the kinetic experiments: (A) pH control system [(1) impulsomat; (2) dosimat; (3) titrator; (4) buret; (5) ammonia solution tank; (6) recorder; (7) pH-meter]; (B) "adsorption vessel" [(1) double-walled, water-jacketed covered vessel; (2) electrode; (3) sampling accessory; (4) magnetic stirrer].

nitrate solution (1 M) were added into the "adsorption vessel". The initial pH of the aforementioned cobalt nitrate solutions was found to be in the range 5–5.5. This was regulated at pH 7.0 before starting the kinetic experiment by adding a suitable amount of the ammonia aqueous solution 0.1 M. Then, the first sampling (1 mL of the solution) was performed.

An amount of γ -alumina powder equal to 0.3 g was then added into the stirred solution. As the adsorption process caused a decrease in pH, the pH control system fed the suspension with the suitable amount of the ammonia solution to keep pH at the value of 7. This amount was recorded for each addition time. A suspension sample equal to 1 mL was taken at various times during the kinetic experiment.

The sampling continued up to the point where a plateau appeared in the curve "amount of the added NH_3 solution vs time". This curve was automatically recorded. The appearance of the plateau indicated that the adsorption process had been practically finished. It is remarkable to note that the higher the initial Co(II) concentration in the impregnating solution the larger the time required to be obtained a plateau in the curve "amount of the added NH_3 solution vs time".

The Co(II) concentration of the impregnating solution was determined photometrically after filtration of suspension samples (1 mL) taken at various times during the kinetic experiment. A Cary 3 Varian spectrophotometer has been used. The determination was based on the Nitrosol R-Salz procedure.⁴⁵ At the end of each kinetic experiment the supernatant was analyzed for Al(III) ionic species (see below experiment B) whereas the suspension was filtered and the solid was dried overnight at 110 °C. XRD patterns were recorded for these solid samples.

The surface Co(II) concentration, actually the concentration of the supported Co(II) (expressed as micromoles of Co(II) per square meter of the support surface area) was calculated from the above determined Co(II) concentrations and taking into account the initial Co(II) concentration in the impregnating solution, the specific surface area and the mass of the support in the sample.

Experiments To Investigate Eventual Surface Dissolution of γ -Alumina (Experiments B and C). An essential prerequisite for the formation of a Co–Al coprecipitate of hydrotalcite structure is the preceding dissolution of the γ -alumina surface and the formation of Al(III) ionic species in the solution, e.g., $\text{Al}(\text{H}_2\text{O})_6^{3+}$. The following two experiments aim to investigate the surface dissolution of γ -alumina under the conditions of

the adsorption kinetics. In the first (experiment B), the supernatant of the suspensions, taken after the end of each kinetic experiment, was analyzed for Al cations using an atomic absorption spectrophotometer (Perkin-Elmer A, Analyst 380). Specifically, we analyzed the supernatants of the suspensions corresponding to the Co(II) solutions with initial concentrations equal to 7×10^{-3} , 10^{-2} , 2×10^{-2} , and 2.5×10^{-2} M used for the kinetic experiments.

Concerning the second experiment (experiment C), a solution of the indifferent electrolyte (NH_4NO_3 0.1 M) was added in the vessel used for the kinetic experiments and the pH was adjusted to seven. Then, 0.3 g of $\gamma\text{-Al}_2\text{O}_3$ powder was added and the eventual change in the pH was monitored for a large time period. The suspension was then filtered, the supernatant was mixed with a Co(II) solution of 10^{-2} M and pH = 7, and the pH was also monitored for a large time period.

The objective of the experiment (C) is to corroborate the results of the experiment (B) concerning the surface dissolution of γ -alumina and the eventual formation of a Co–Al mixed phase of hydrotalcite structure. In fact, the surface dissolution of γ -alumina is expected to cause a change in pH, initially adjusted to seven. Moreover, in the case where even a very small amount of the Al(III) ionic species were present in the supernatant, these are expected to react with the $\text{Co}(\text{H}_2\text{O})_6^{2+}$ ions causing a change in the solution pH.

Reversibility Experiment (Experiment D). To formulate the kinetics of deposition of the $\text{Co}(\text{H}_2\text{O})_6^{2+}$ ions on the γ -alumina surface, it was necessary to estimate the contribution of the desorption to the whole deposition process.

To do that, we have titrated, from pH ≈ 2 to pH ≈ 12 and then from pH ≈ 12 back to pH ≈ 2 , an impregnation Co(II) solution 10^{-2} M in Co(II) with volume equal to 100 mL. Moreover, we have titrated, from pH ≈ 4 to pH ≈ 11.5 and then from pH ≈ 11.5 back to pH ≈ 4 , the corresponding Co(II) suspension containing 0.5 g of γ -alumina. The titrations have been performed at 25 °C.

X-ray Powder Analysis (XRD). The X-ray diffraction patterns of the dried solids (taken after the end of the kinetics experiments) were recorded in the range 10–80° (scanning rate: $0.6^\circ \text{ min}^{-1}$) by a Philips PW 1480 automated diffractometer using the Cu $K\alpha$ ($\lambda = 1.4518 \text{ \AA}$) radiation filtered through Ni.

Results and Discussion

On the Eventual Dissolution of the γ -Alumina Surface and the Formation of a Co–Al Coprecipitate of Hydrotalcite Structure during the Kinetic Experiments. The atomic absorption analysis performed after each kinetic experiment (experiment B) showed the absence of aluminum species in the supernatant. Moreover, in the experiment C, the pH of the suspension of the indifferent electrolyte remained constant for large time. This was also observed for the solution prepared by mixing the corresponding supernatant with the cobalt nitrate solution (experiment C).

The above show that the surface dissolution of the γ -alumina and the formation of a Co–Al hydrotalcite complex, if any, is not the predominant deposition process under conditions where our kinetic experiments have been performed. The above conclusion is corroborated by the XRD patterns recorded for the dried samples. In fact, these patterns reveal in all cases the crystal structure of the γ -alumina but not the formation of a Co supported phase of Co–Al hydrotalcite crystal structure, even for the sample with the maximum surface Co(II) concentration ($13.2 \mu\text{mol m}^{-2}$) corresponding to 4 theoretical $\text{Co}(\text{H}_2\text{O})_6^{2+}$ surface layers, as may be seen by inspecting Figure 2. The

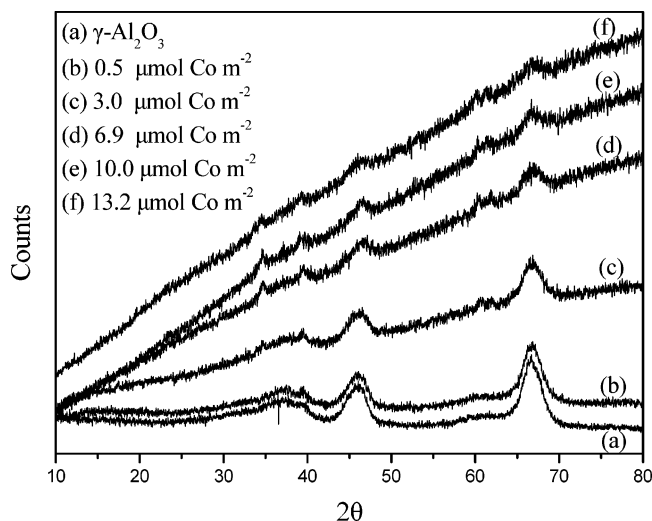


Figure 2. X-ray powder diffraction patterns for a few dried Co(II) supported γ -alumina samples with different Co(II) surface concentrations. The XRD pattern of γ -alumina is also presented.

decrease of the magnitude of the γ -alumina diffraction peaks with the amount of the supported cobalt species may be attributed to two reasons: first is the dilution of the sample with respect to the support, and second is the increasing signal of the baseline due to the Co fluorescence.

One can imagine two reasons for justifying the disagreement observed between our results and those of Pauliac et al.²³ and Caillerie et al.²⁴ The first is related to the difference in the Co(II) species deposited, $\text{Co}(\text{NH}_3)_6^{2+}$, instead of $\text{Co}(\text{H}_2\text{O})_6^{2+}$, and the second is related to the particular surface characteristics of the γ - Al_2O_3 used in each case. However, we have recently calculated the magnitude of the γ -alumina surface dissolution using the Caillerie results.⁴² This calculation showed that even in that case 0.005 wt % Al initially belonging to γ -alumina had been dissolved.

Finally, it seems to us useful to point out that EXAFS results have shown that there is no considerable diffusion, if any, of Co(II) ions into the γ -alumina lattice during deposition.²² Therefore, the total amount of the deposited cobalt should be considered to be supported on the γ -alumina surface.

On the Reversibility of the Adsorption Process. The results of the reversibility experiment (experiment D) are illustrated in Figure 3. Concerning the $\text{Co}(\text{NO}_3)_2$ aqueous solution the results are quite expectable. The addition of aliquots of the basic solution increases the pH from 2 to ≈ 8 . In this pH range the solution is stable in agreement with the literature.^{46–52} The addition of small volumes of the basic solution, which corresponds to the horizontal part of curve a, causes the formation of the $\text{Co}(\text{OH})\text{NO}_3$ and then of the $\text{Co}(\text{OH})_2$ precipitate. This is manifested by the change of the color from pink to green-blue and then to gray-black. The end of precipitation is indicated by the additional increase in pH from 8 to 12. The inverse titration procedure of the solution provided similar though not identical curve (curve b).

The situation changes completely when we go from the solution to the suspension (curves c and d). First it may be observed that the first part of the curve (c) is not so abrupt as the corresponding part of curve a. This is due to the low extent of the Co(II) adsorption in the pH range 4–6, which causes the release of small amounts of H^+ ions. At pH ≈ 6 the extent of adsorption increases, in agreement with the literature,^{20,21,25–27,39} bringing about a drastic decrease in the slope of curve c up to pH ≈ 8 where the adsorption is accomplished. Thus, the almost

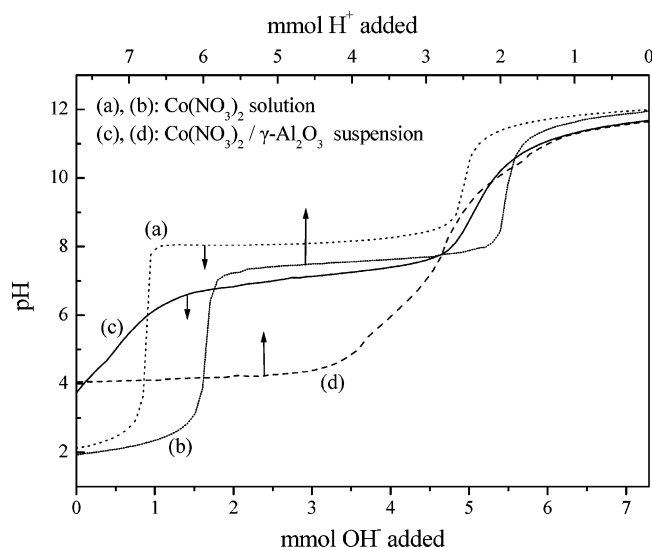


Figure 3. Titration curves of both a cobalt nitrate solution of 10^{-2} M and volume equal to 100 mL (curves a and b) and the corresponding impregnating suspension containing 0.5 g of γ -alumina (curves c and d).

horizontal part of curve c corresponds to the adsorption process. This process keeps the pH quite low, inhibiting the formation in the bulk solution of the above-mentioned solid Co phases. This is manifested by the fact that it was not observed any change in the pink color of the suspension during impregnation.

Going from the adsorption (c) to the desorption (d) curve, it may be observed that the shapes of these curves are extremely different. More precisely, curve d appears an almost constant slope in the pH range 10–4. This indicates that a portion of the adsorbed Co(II) species is progressively desorbed. However, the most important observation of this set of experiments is that the almost horizontal part of curve d, reasonably corresponding to the main desorption process, appears at pH values much less than those corresponding to the adsorption process (horizontal part of curve c). The so formed hysteresis loop, reported for the first time to the extent of our knowledge, presumably imply that the desorption process is significantly slower than adsorption. A portion of the Co(II) adsorbed species remains on the support surface at pH values higher than 5. Presumably, these strongly bounded Co(II) supported species are related with the inner sphere surface Co(II) mononuclear or oligonuclear complexes which have one or more surface oxygens as common ligands.

The findings presented in this section suggest that desorption is significantly slower than adsorption. The same conclusion has been recently drawn with respect to the desorption of the deposited Co(II) species on anatase surface, on the basis of a work which is now in progress. The above will help us to formulate the deposition kinetics.

Kinetics of Deposition: The Promotive Action of the Deposited Co(II) Species. As already mentioned in the Introduction, the study of the kinetics of deposition of the $\text{Co}(\text{H}_2\text{O})_6^{2+}$ species on the “electrolytic solution/ γ -alumina interface” is the main goal of the present work. The results drawn from the kinetic experiments, described in the experimental part, allowed us to investigate the variation with time of the Co(II) concentration in the impregnating solution. Although the details of this variation depends on the initial Co(II) concentration, $C_{\text{Co,init}}$ (5×10^{-4} , 7×10^{-4} , 10^{-3} , 3×10^{-3} , 5×10^{-3} , 7×10^{-3} , 9×10^{-3} , 10^{-2} , 2×10^{-2} , and 2.5×10^{-2} M), three rather typical kinetic curves corresponding to a low (5×10^{-4}

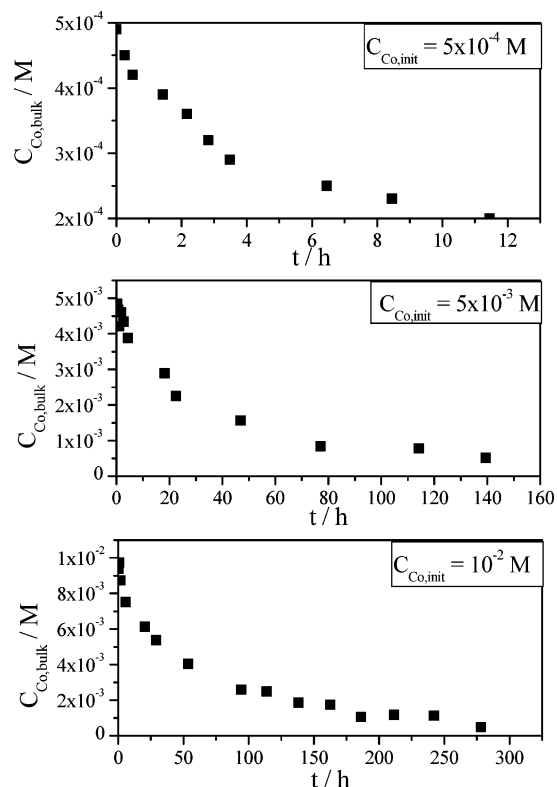


Figure 4. Typical kinetic curves for deposition of the $\text{Co}(\text{H}_2\text{O})_6^{2+}$ ions on the “electrolytic solution/ γ -alumina” interface corresponding to a low (5×10^{-4} M), medium (5×10^{-3} M), and high (10^{-2} M) initial Co(II) concentration in the impregnating solution. Experimental conditions: pH = 7, 25 °C, $I = 0.1$ M, volume of impregnating solution = 150 mL, and mass of γ -alumina = 0.3 g.

M), medium (5×10^{-3} M) and high (10^{-2} M) $C_{\text{Co,init}}$ are illustrated in Figure 4. It may be observed that the time required in order to approach equilibrium increases considerably with the initial Co(II) concentration in the impregnating solution.

Assuming that the last point of the kinetic curves corresponded to the equilibrium, we calculated the surface concentration of the adsorbed Co(II) for each Co(II) concentration determined in the supernatant, $C_{\text{Co,eq}}$, at the end of each kinetic experiment. The so determined deposition isotherm is illustrated in Figure 5. Since our principal goal was the study of the deposition kinetics and not the deposition thermodynamics, the deposition isotherm determined does not involve a sufficient number of points, mainly for high $C_{\text{Co,eq}}$ values. Therefore, we did not attempt its mathematical analysis. Nevertheless, two observations are actually remarkable: First, the appearance of a plateau at the isotherm is in disagreement with a mechanism of surface-support dissolution, subsequent formation of Co–Al phase of hydrotalcite structure and its deposition on the support surface. Second, the form of the isotherm at low and medium Co(II) equilibrium concentrations, where the sufficient number of the experimental points allows one to observe a slight increase in the extent of adsorption followed by an abrupt increase as the value of the $C_{\text{Co,eq}}$ increases.

We have observed several times in the past this “S” type of deposition isotherms with respect to the adsorption of transition metal oxyanions on the γ -alumina surface. We have attributed these observations to the development of attractive lateral interactions between the adsorbed species.^{53–55} Concerning the deposition of the $\text{Co}(\text{H}_2\text{O})_6^{2+}$ species it seems to us reasonable to attribute the sigmoidal character of the deposition isotherm to the promotive action of the already sorbed Co(II) species.

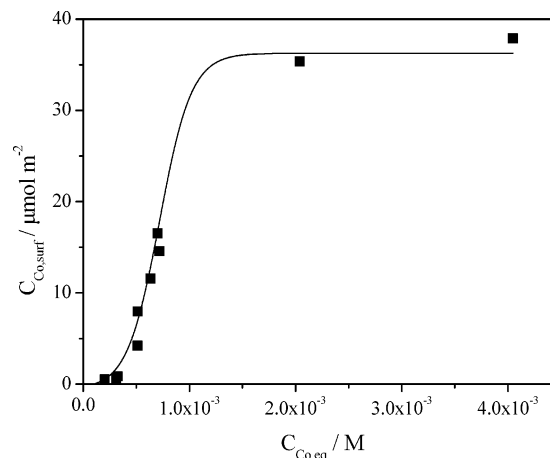
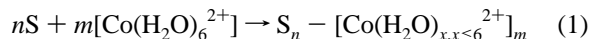


Figure 5. Deposition isotherm of the $\text{Co}(\text{H}_2\text{O})_6^{2+}$ ions on the “electrolytic solution/ γ -alumina” interface. The experimental conditions are reported in the legend of Figure 4.

This action may be responsible for the formation of the multinuclear surface complexes and for the formation of the surface Co(II) precipitates, for relative high Co(II) surface concentration. This is in full agreement with the literature, mainly with the electronic microscopy and EXAFS results.^{22,30}

Kinetics of Deposition: Development of the Methodology.

To formulate the deposition of the $\text{Co}(\text{H}_2\text{O})_6^{2+}$ ions, we assume negligible surface dissolution of the adsorbent and negligible participation of desorption to the deposition kinetics, in agreement with the findings presented previously. The second assumption will be tested from the kinetic results. On the basis of these assumptions we consider that the deposition process is described by the following chemical equation:



According to the above chemical equation m ions of cobalt aqua complex are deposited on n surface sites forming the inner sphere complexes illustrated in the rhs of equation. The well-known releasing of the H^+ ions from the surface and the decrease of the water ligands of Co(II) are not illustrated in the rhs of the equation.

Assuming that the above equation is time-independent we may write-down the following kinetic expression:

$$r_{\text{Co,bulk}} = -\frac{dC_{\text{Co,bulk}}}{dt} = kC_{\text{Co,bulk}}^m C_S^n \quad (2)$$

In the above expression by $r_{\text{Co,bulk}}$, $C_{\text{Co,bulk}}$, C_S , and k , we denote respectively, the rate of consumption of the $\text{Co}(\text{H}_2\text{O})_6^{2+}$ species in the bulk solution, the concentration of these species in the bulk solution, the concentration of the surface sites, and the reaction rate constant. The final goal of the kinetics is, of course, the determination of the parameters k , m , and n by fitting eq 2 to the experimental values $r_{\text{Co,bulk}}$ vs $C_{\text{Co,bulk}}$. This is expected to enable us to approach to the local structure of the inner sphere surface complexes formed. However, this is not so easy because the “reaction” resulting to deposition takes place inside the interfacial region and not in the bulk solution. This means that the rate constant mentioned above is apparent. The following relationships allow the relating of the bulk with the surface cobalt concentration:

$$C_{\text{Co,bulk}} = C_{\text{Co,init}} - C_{\text{Co,surf}} \quad (3)$$

$$C_{\text{Co,surf}} = C_{\text{Co,bulk}} \exp(-zF\Psi/RT) \quad (4)$$

In the above expressions by $C_{\text{Co,init}}$, $C_{\text{Co,surf}}$, z , F , Ψ , R , and T , we symbolize respectively the initial bulk concentration, the surface cobalt concentration, the charge of the cobalt aqua complex (+2), the Faraday constant, the potential in the interfacial region, the gas constant, and the absolute temperature of deposition. The first expression is a mass-balance equation whereas the second is the well-known Boltzman equation. Taking into account that $C_{\text{Co,init}}$ is constant, the differentiation of eq 3 with respect to the time provides the relationship between the bulk and surface deposition rate:

$$r_{\text{Co,bulk}} = -\frac{dC_{\text{Co,bulk}}}{dt} = \frac{dC_{\text{Co,surf}}}{dt} \quad (5)$$

By combining the eq 2 with eqs 4 and 5, the following expression may be derived:

$$r_{\text{Co,bulk}} = -\frac{dC_{\text{Co,bulk}}}{dt} = \frac{dC_{\text{Co,surf}}}{dt} = k_{\text{intr}} \exp(-mzF\Psi/RT) C_{\text{Co,bulk}}^m C_{\text{S}}^n \quad (6)$$

Since the above expression describes the deposition kinetics in the interfacial region, the rate constant, k_{intr} , of this equation is an intrinsic one. This is, of course, related with the apparent rate constant of eq 2. Unfortunately eq 6 does not allow the determination of the exponential parameters m and n . This is because the interfacial potential and the concentration of the surface sites are unknown. Moreover, the interface potential changes with the concentration of the deposited Co(II) surface species. Thus, the only way to overcome this problem is to attempt the fitting of eq 6 to the experimental data under conditions where the interface potential; thus, the factor $\exp(-mzF\Psi/RT)$ and the concentration of the surface sites are constant. In other words, it is necessary to attempt the aforementioned fitting for constant Co(II) surface concentration. Under these conditions, eq 6 is transformed into eq 7:

$$r_{\text{Co,bulk}} = -\frac{dC_{\text{Co,bulk}}}{dt} = \frac{dC_{\text{Co,surf}}}{dt} = k' C_{\text{Co,bulk}}^m \quad (7)$$

where the apparent rate constant k' is equal to the product $k_{\text{intr}} \exp(-mzF\Psi/RT) C_{\text{S}}^n$. It is obvious that using eq 7 we would determine only the value of m and the value of the apparent rate constant k' . To do that we have adopted the following three-step procedure using the software Microcal Origin Version 6.0.

In the first step we calculated the kinetic curves, for each initial Co(II) concentration in the bulk solution, obtaining the best fitting to the experimental points " $C_{\text{Co,bulk}}$ vs time" determined in each one of the experiments A (e.g., Figure 6). In the second step and using the computer program we calculated the derivatives $-(dC_{\text{Co,bulk}}/dt)$ for each value of $C_{\text{Co,bulk}}$. This allowed the construction of the differential kinetic curves (e.g., Figure 7). In the third step we selected a $C_{\text{Co,surf}}$ value and for various values of $C_{\text{Co,init}}$ we calculated the corresponding $C_{\text{Co,bulk}}$ values using eq 3. Then, using Figure 7, we determined the values of the rate corresponding to the above-mentioned values of $C_{\text{Co,bulk}}$. This procedure allowed the determination of the values for the pair $(r_{\text{Co,bulk}}, C_{\text{Co,bulk}})$ which correspond to a given Co(II) surface concentration. In the final step of the procedure, we attempted to fit the values of the aforementioned pair of parameters to eq 7.

In all cases the best fitting was obtained for $m \cong 2$. Figure 8 illustrates the fitting achieved for several values of the Co(II) surface concentration. Inspection of this figure shows that in all cases the line passes practically through zero. This observa-

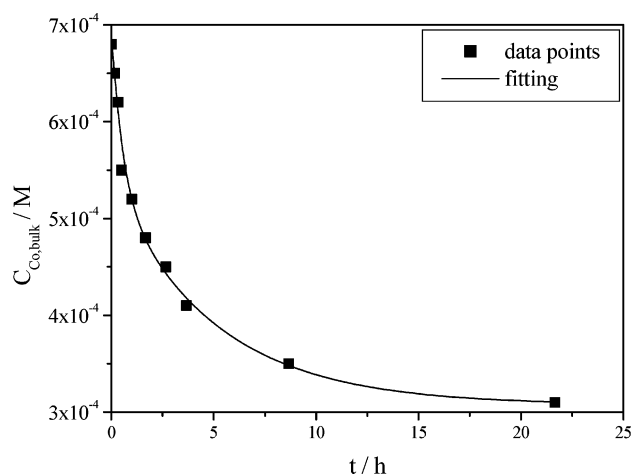


Figure 6. Variation of the Co(II) concentration in the impregnating solution, $C_{\text{Co,bulk}}$, with time. $C_{\text{Co,init}} = 7 \times 10^{-4}$ M. The experimental conditions are reported in the legend of Figure 4.

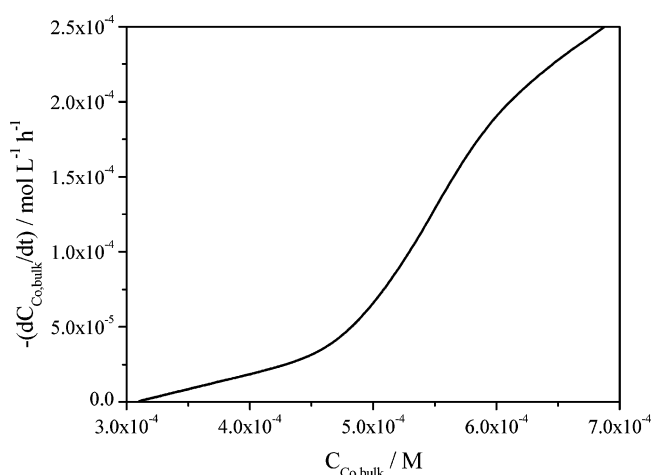


Figure 7. Variation of the rate of disappearance of the $\text{Co}(\text{H}_2\text{O})_6^{2+}$ ions from the impregnating solution, $-dC_{\text{Co,bulk}}/dt$, with the concentration in the impregnating solution, $C_{\text{Co,bulk}}$.

tion is in full agreement with the assumption done that desorption does not significantly participate to the whole deposition kinetics. It is rather unexpected but the same value of m was achieved irrespectively of the Co(II) surface concentration in the range of 0.03 to 6 theoretical $\text{Co}(\text{H}_2\text{O})_6^{2+}$ surface layers. Therefore, eq 7 may be transformed into eq 8.

$$r_{\text{Co,bulk}} = -\frac{dC_{\text{Co,bulk}}}{dt} = \frac{dC_{\text{Co,surf}}}{dt} = k' C_{\text{Co,bulk}}^2 \quad (8)$$

Kinetics of Deposition: Investigating the Local Structure of the Surface Co(II) Species. The above findings, the most important of the present work, allow us to approach to the local structure of the inner sphere Co(II) surface complexes formed, at least from the side of the interface. In fact, one may imagine that the chemical eq 1 describes indeed the real deposition process and that two $\text{Co}(\text{H}_2\text{O})_6^{2+}$ ions are involved in the reaction with the surface reception sites. It is quite probable that the deposition step involves the simultaneous adsorption and the dimerization of two interfacial $\text{Co}(\text{H}_2\text{O})_6^{2+}$ ions through (hydr)oxobridges. The later is not unexpected if one takes into account that the dimerization involves the releasing of protons and their removal from the interfacial region. This partially compensates the increase of the positive interface potential brought about due to the adsorption of the positive $\text{Co}(\text{H}_2\text{O})_6^{2+}$

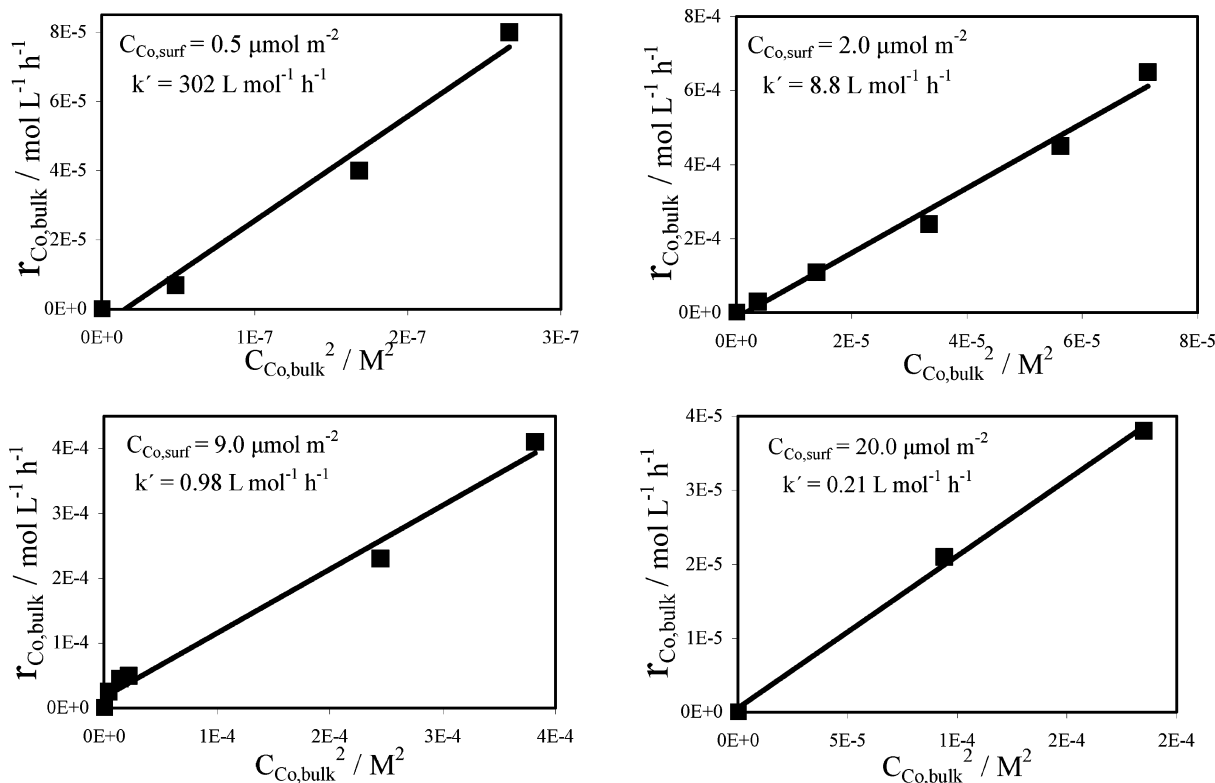


Figure 8. Plots of eq 8 for various values of the surface Co(II) concentration. The values of this parameter and the values of the apparent rate constant, k' , of eq 8 are illustrated.

TABLE 1: Values of the Apparent Rate Constant, k' , Achieved by Fitting Eq 8 to the Experimental Data, for Various Values of the Surface Co(II) Concentration

$C_{\text{Co,surf}}/\mu\text{mol Co(II) m}^{-2}$	$k'/\text{L mol}^{-1} \text{h}^{-1}$
0.1	448 ± 84
0.3	388 ± 65
0.5	302 ± 32
0.7	179 ± 24
1.0	13 ± 1
1.5	10.2 ± 0.7
2.0	8.8 ± 0.5
3.0	8.5 ± 0.3
5.0	1.43 ± 0.04
7.0	1.08 ± 0.04
9.0	0.98 ± 0.06
12	0.76 ± 0.07
15	0.16 ± 0.02
20	0.21 ± 0.01

species. In this point it should be noted that at $\text{pH} \approx 7$, where the deposition takes place, the γ -alumina surface is positively charged bringing about a development of positive surface potential in the interface. A remarkable point is that kinetics may discover the interfacial dimerization during deposition even at too low Co(II) surface concentration, namely at $0.1 \mu\text{mol Co(II) m}^{-2}$ corresponding to 0.03 theoretical $\text{Co(H}_2\text{O)}_6^{2+}$ surface layers.

In Table 1, we illustrate the values for the apparent rate constant, k' , achieved by fitting eq 8 to the experimental data, for various values of the surface Co(II) concentration. From this table it may be seen that k' decreases with the surface Co(II) concentration. The interpretation of this observation is quite difficult because k' depends on three factors ($k' = k_{\text{intr}} \cdot \exp(-mzF\Psi/RT) \cdot C_s^n$) among which only the first, k_{intr} , is considered to be constant. The variable in the second factor is the positive interface potential Ψ . This is expected to increase with the increase of the Co(II) surface concentration bringing about an exponential decrease of the Boltzman factor with this parameter.

As to the third factor, C_s^n , the situation is much more complicated because the exact nature of the reception sites and the value of n are for the moment unknown. In fact, if one considers that only the surface hydroxyls of γ -alumina constitute the reception sites, which is much probable in too low values of the surface Co(II) concentration, a decrease of the C_s^n value with the surface Co(II) concentration is expected. However, if one takes into account the promotive action of the already deposited Co(II) species, inferred by spectroscopy and presumably from the S form of the deposition isotherm, the above-mentioned decrease may be under or over compensated. The reason is that in this case the reception sites may involve, in addition, surface hydroxyls of the already deposited Co(II) surface species.

To investigate further this quite difficult point we speculate that as the surface Co(II) concentration increases and thus the number of the γ -alumina surface hydroxyls decreases, more and more of surface hydroxyls of the already formed surface Co(II) species participate to the creation of the reception sites. In such a case the factor C_s^n of the rhs of eq 6 is expected to change slightly as it is compared to the monotonic decrease of the exponential factor $\exp(-mzF\Psi/RT)$. Alternatively, even in the case where the above picture is not realistic, the factor C_s^n would be, again, considered to be practically constant as it is compared to the exponential factor. This is because, at least for low Co(II) surface concentration, the number of the reception sites in the suspension is at least 1 order of magnitude greater than the number of the $\text{Co(H}_2\text{O)}_6^{2+}$ ions. Therefore, a zero order kinetics with respect to the surface sites seems to be reasonable. Moreover, we assume that the interface positive potential Ψ increases almost linearly with the surface Co(II) concentration. Taking into account the above assumptions, the fact that k_{intr} is actually constant and the value of the interface potential is not far from zero at $\text{pH} = 7$ (pzc of γ -alumina is equal to 7.5), the relationship $k' = k_{\text{intr}} \cdot \exp(-mzF\Psi/RT) \cdot C_s^n$ may be reduced to

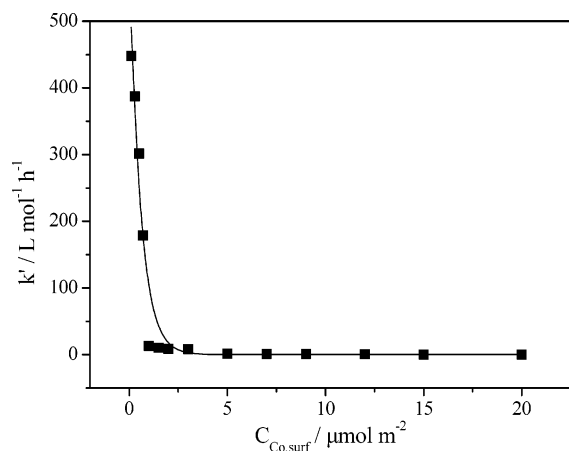


Figure 9. Fitting achieved for the data “ k' vs $C_{\text{Co,surf}}$ ” compiled in Table 1 to the expression $k' = a \cdot \exp(-bC_{\text{Co,surf}})$.

the relationship $k' = a \cdot \exp(-bC_{\text{Co,surf}})$, where $a = k_{\text{intr}} \cdot C_s^n$ and $b = mZF\Psi/RT$ are constant.

To test the above-mentioned assumptions we tried to fit the data illustrated in Table 1 to the above-mentioned reduced relationship. Inspection of Figure 9 shows that a quite good fitting is obtained corroborating, presumably, the above assumptions. The next step in our kinetic analysis was the calculation of the proportionality constant, c , of the adopted linear relation

$$\Psi = c \cdot C_{\text{Co,surf}} \quad (9)$$

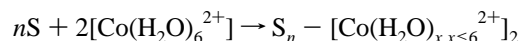
This was easily achieved taking into account that $c = bRT/2zF$. The thus determined value of c allowed the calculation of the interface potential, through eq 9, for each Co(II) surface concentration. The thus calculated values of Ψ were on the order of millivolts which are very reasonable as they are compared to the values of the interface potential usually determined for oxides on the basis of the electrostatics and thermodynamics. The above corroborate further the assumptions done previously concerning the predominant influence of the Boltzmann factor on the variation of the apparent rate constant k' .

Conclusions

From the present work the following conclusions may be drawn.

1. The deposition kinetics of the Co(II) ions on the γ -alumina surface may be described by the following expression $r_{\text{Co,bulk}} = k' C_{\text{Co,bulk}}^2$.

2. The above-mentioned kinetic expression may be derived assuming the following deposition scheme:



3. The above expressions indicate that two $\text{Co}(\text{H}_2\text{O})_6^{2+}$ ions are involved, from the side of the interface, in the reaction with the reception sites. It is quite probable that the deposition step involves the simultaneous adsorption and dimerization of the two interfacial $\text{Co}(\text{H}_2\text{O})_6^{2+}$ ions through (hydr)oxobridges.

4. The S form of the deposition isotherm and the dependence of the apparent rate constant, k' , on the surface Co(II) concentration suggest that the already deposited Co(II) species may be involved in the reception sites, S, promoting the adsorption and resulting to the formation of multinuclear inner sphere complexes and then to Co(II) surface precipitates.

5. At pH 7 and room temperature, where the deposition was taken place, the dissolution of the γ -alumina surface is negligible even in the presence of the $\text{Co}(\text{H}_2\text{O})_6^{2+}$ species in the impregnating solution.

6. It was inferred that desorption does not participate significantly to the whole deposition process. Reasonable for oxides interface potential values were determined for the first time using kinetic results.

7. The findings of the present kinetic study, our recent spectroscopic results⁵⁶ as well as unpublished results concerning mainly the Co(II)/H⁺ exchange ratio are expected to help us to shed more light on the local structure of the deposited Co(II) species under various conditions. On the other hand, we have already taken advantage of the present kinetic results to prepare by EDF Co/ γ - Al_2O_3 catalysts with very high dispersion of the supported Co species.⁵⁷ These catalysts were found to be very active in the complete oxidation of benzene.⁵⁷

Acknowledgment. The Research Committee of the University of Patras is gratefully acknowledged for providing the financial support for this work (research program: Karath-eodory).

References and Notes

- (1) Liotta, L. F.; Pantaleo, G.; Macaluso, A.; Di Carlo, G.; Deganello, G. *Appl. Catal., A: Gen.* **2003**, *245*, 167.
- (2) Horiuchi, T.; Fujiwara, T.; Chen, L.; Suzuki, K.; Mori, T. *Catal. Lett.* **2002**, *78*, 319.
- (3) Nanba, T.; Uemura, A.; Ueno, A.; Haneda, M.; Hamada, H.; Kakuta, N.; Miura, H.; Ohfun, H.; Udagawa, Y. *Bull. Chem. Soc. Jpn.* **1998**, *71*, 2331.
- (4) Torncrona, A.; Skoglundh, M.; Thormahlen, P.; Fridell, E.; Jobson, E. *Appl. Catal., B: Environ.* **1997**, *14*, 131.
- (5) Thomson, J. *Catal. Lett.* **1996**, *40*, 119.
- (6) Okamoto, Y.; Adachi, T.; Nagata, K.; Odawara, M.; Imanaka, T. *Appl. Catal.* **1991**, *73*, 249.
- (7) El-Shobaky, G. A.; Fagal, G. A.; Saber, T. M. H. *Bull. Soc. Chim. Fr.* **1987**, 547.
- (8) Hernadi, K.; Fonseca, A.; Piedigrosso, P.; Delvaux, M.; Nagy, J. B.; Bernaerts, D.; Riga, J. *Catal. Lett.* **1997**, *48*, 229.
- (9) Bailie, J. E.; Rochester, C. H.; Hutchings, G. J. *J. Chem. Soc., Faraday Trans.* **1997**, *93*, 4389.
- (10) Lapidus, A.; Krylova, A.; Rathousky, J.; Zukal, A.; Jancalkova, M. *Appl. Catal., A: General* **1992**, *80*, 1.
- (11) Ho, S. W.; Houalla, M.; Hercules, D. M. *J. Phys. Chem.* **1990**, *94*, 6396.
- (12) Nitta, Y.; Ueno, K.; Imanaka, T. *Appl. Catal.* **1989**, *56*, 9.
- (13) Lycourghiotis, A. *Preparation of Catalysts VI*; Poncelet, G.; Martens, J.; Delmon, B.; Jacobs, P. A.; Grange, P., Eds.; Elsevier: Amsterdam, 1995; p 95.
- (14) Karakostas, L.; Matralis, H. K.; Kordulis, Ch.; Lycourghiotis, A. *J. Catal.* **1996**, *162*, 306.
- (15) Papadopoulou, Ch.; Karakostas, L.; Matralis, H. K.; Kordulis, Ch.; Lycourghiotis, A. *Bull. Soc. Chim. Belg.* **1996**, *105*, 247.
- (16) Georgiadou, I.; Papadopoulou, Ch.; Matralis, H. K.; Voyiatzis, G. A.; Lycourghiotis, A.; Kordulis, Ch. *J. Phys. Chem. B* **1998**, *102*, 8459.
- (17) Kordulis, Ch.; Lappas, A. A.; Fountzoula, Ch.; Drakaki, K.; Lycourghiotis, A.; Vasalos, I. A. *Appl. Catal., A: Gen.* **2001**, *209*, 85.
- (18) Lycourghiotis, A.; Kordulis, Ch.; Bourikas, K. *Encycl. Surf. Colloid Sci.* **2002**, 1366.
- (19) Vakros, J.; Bourikas, K.; Kordulis, Ch.; Lycourghiotis, A. *J. Phys. Chem. B* **2003**, *107*, 1804.
- (20) Tewari, P. H.; Campell, A. B.; Lee, W. *Can. J. Chem.* **1972**, *50*, 1642.
- (21) Tewari, P. H.; Lee, W. *J. Colloid Interface Sci.* **1975**, *52*, 77.
- (22) Chisholm-Brawse, C. J.; O'Day, P. A.; Brown, G. E., Jr.; Parks, G. A. *Nature (London)* **1990**, *348*, 528.
- (23) Pauliac, J. L.; Clause, O. *J. Am. Chem. Soc.* **1993**, *115*, 11602.
- (24) Caillerie, J. B. E.; Karmarec, M.; Clause, O. *J. Am. Chem. Soc.* **1995**, *117*, 1147.
- (25) Vordonis, L.; Spanos, N.; Koutsoukos, P.; Lycourghiotis, A. *Langmuir* **1992**, *8*, 1736.
- (26) Spanos, N.; Lycourghiotis, A. *J. Chem. Soc., Faraday Trans.* **1993**, *89*, 4101.
- (27) Vakros, J.; Kordulis, Ch.; Lycourghiotis, A. *Langmuir* **2002**, *18*, 417.

- (28) Katz, L. E.; Hayes, K. F. *J. Colloid Interface Sci.* **1995**, *170*, 477.
- (29) Katz, L. E.; Hayes, K. F. *J. Colloid Interface Sci.* **1995**, *170*, 491.
- (30) Towle, S. N.; Bargar, J. R.; Brown, G. E., Jr.; Parks, G. A. *J. Colloid Interface Sci.* **1997**, *187*, 62.
- (31) Towle, S. N.; Bargar, J. R.; Brown, G. E., Jr.; Parks, G. A. *J. Colloid Interface Sci.* **1999**, *217*, 312.
- (32) James, R. O. Ph.D. Dissertation, University of Melbourne, 1971.
- (33) James, R. O.; Healy, T. W. *J. Colloid Interface Sci.* **1972**, *40*, 42.
- (34) James, R. O.; Healy, T. W. *J. Colloid Interface Sci.* **1972**, *40*, 53.
- (35) O'Day, P. A.; Chisholm-Browse, C. J.; Towle, S. N.; Parks, G. A.; Brown, G. E., Jr. *Geochim. Cosmochim. Acta* **1996**, *60*, 2515.
- (36) Towle, S. N.; Brown, G. E., Jr.; Parks, G. A. *J. Colloid Interface Sci.* **1999**, *217*, 299.
- (37) Dugger, D. L.; Stanton, J. H.; Irby, B. N.; McConnell, B. L.; Curings, W. W.; Maatmen, R. W. *J. Phys. Chem.* **1964**, *68*, 757.
- (38) Bye, G. C.; McEvoy, M.; Malati, M. A. *J. Chem. Soc., Faraday Trans.* **1983**, *79*, 2311.
- (39) Tamura, H.; Katayama, N.; Furuichi, R. *J. Colloid Interface Sci.* **1997**, *195*, 192.
- (40) Agashe, K. B.; Regalbuto, J. R. *J. Colloid Interface Sci.* **1997**, *185*, 174.
- (41) Hao, X.; Spieker, W. A.; Regalbuto, J. R. *J. Colloid Interface Sci.* **2003**, *267*, 259.
- (42) Bourikas, K.; Kordulis, Ch.; Vakros, J.; Lycourghiotis, A. *Adv. Colloid Interface Sci.* **2004**, *110*, 97.
- (43) Hiemstra, T.; Van Riemsdijk, W. H. *J. Colloid Interface Sci.* **1996**, *179*, 488.
- (44) Hiemstra, T.; Van Riemsdijk, W. H. *J. Colloid Interface Sci.* **1999**, *210*, 182.
- (45) Samdell, E. B. *Colorimetric Determination of Traces of Metals*; Interscience: New York, 1950; p 274.
- (46) D'Angelo, P.; Barone, V.; Chillemi, G.; Sanna, N.; Meyer-Klaucke, W.; Pavel, N. V. *J. Am. Chem. Soc.* **2002**, *124*, 1958.
- (47) Baes, C. F. Jr.; Mesmer, R. E. *The Hydrolysis of Cations*; Wiley: New York, 1976.
- (48) Smith, R. M.; Martell, A. E. *Critical Stability Constants*; Plenum: New York, 1981; Vol. 4.
- (49) Magini, M.; Licheri, G.; Paschina, G.; Piccaluga, G.; Pinna, G. *X-ray Diffraction of Ions in Aqueous Solutions: Hydration and Complex Formation*; CRC Press: Boca Raton, FL, 1988.
- (50) Ohtaki, H.; Radnai, T. *Chem. Rev.* **1993**, *93*, 1157.
- (51) Enderby, J. E. *Chem. Soc. Rev.* **1995**, *24*, 159.
- (52) Marcus, Y. *Chem. Rev.* **1988**, *88*, 1475.
- (53) Spanos, N.; Vordonis, L.; Kordulis, Ch.; Koutsoukos, P.; Lycourghiotis, A. *J. Catal.* **1990**, *124*, 315.
- (54) Karakostas, L.; Kordulis, Ch.; Lycourghiotis, A. *Langmuir* **1992**, *8*, 1318.
- (55) Spanos, N.; Lycourghiotis, A. *Langmuir* **1993**, *9*, 2250.
- (56) Vakros, J.; Bourikas, K.; Perlepes, S.; Kordulis, Ch.; Lycourghiotis, A. *Langmuir* **2004**, *20*, 10542.
- (57) Ataloglou, T.; Vakros, J.; Bourikas, K.; Fountzoula, Ch.; Kordulis, Ch.; Lycourghiotis, A. *Appl. Catal., B: Environ.* **2004**, *57*, 297.